

Spotty calcification and plaque vulnerability *in vivo*: frequency-domain optical coherence tomography analysis

Yu Kataoka¹, Rishi Puri^{2,3}, Muhammad Hammadah³, Bhanu Duggal³, Kiyoko Uno³, Samir R. Kapadia³, E. Murat Tuzcu³, Steven E. Nissen³, Stephen J. Nicholls¹

¹South Australian Health & Medical Research Institute, University of Adelaide, Adelaide, Australia; ²Cleveland Clinic Coordinating Center for Clinical Research, Cleveland, Ohio, USA; ³Department of Cardiovascular Medicine, Heart & Vascular Institute, Cleveland Clinic, Cleveland, Ohio, USA

Correspondence to: Yu Kataoka, MD. South Australian Health & Medical Research Institute, North Terrace, Adelaide, SA 5001, Australia. Email: jimmyk67@yahoo.co.jp.

Background: Spotty calcification is a morphological characteristic of a vulnerable plaque phenotype. While this calcium pattern is considered an active process, promoted by inflammation, it is unknown whether spotty calcification associates with development of microstructures observed in vulnerable plaques. As frequency-domain optical coherence tomography (FD-OCT) enables visualization of microstructures associated with plaque vulnerability, we investigated the association between spotty calcification and plaque microstructures by using FD-OCT.

Methods: A total of 300 patients with stable coronary artery disease (CAD), having clinical indication for percutaneous coronary intervention (PCI), were analyzed. Totally 280 non-culprit lipid plaques within the target vessel requiring PCI were evaluated by FD-OCT. Spotty calcification was defined as a presence of lesion <4 mm in length, containing an arc of calcification <90° on FD-OCT. Plaque microstructures were compared in non-culprit lipid-rich plaques with and without spotty calcification.

Results: Spotty calcification was observed in 39.6% of non-culprit lipid-rich plaques, with 30.6% of these plaques demonstrating multiple spotty calcifications. Plaques containing spotty calcification exhibited a greater lipid index (= averaged lipid arc × lipid length); 1,511.8±1,522.3 vs. 815.2±1,040.3 mm°, P<0.0001), thinner fibrous caps (89.0±31.6 vs. 136.5±32.5 μm, P=0.002) and a higher prevalence of microchannels (45.9% vs. 17.7%, P=0.007). A significant association was observed between the number of spotty calcifications per plaque and fibrous cap thickness (r=-0.40, P=0.006). Increased number of spotty calcification was also associated with a higher prevalence of microchannel within plaques (P=0.01).

Conclusions: In patients with stable CAD requiring PCI, the presence of spotty calcification imaged by FD-OCT was associated with features of greater plaque vulnerability.

Keywords: Calcification; plaque vulnerability; optical coherence tomography; plaque

Submitted Nov 18, 2014. Accepted for publication Nov 26, 2014.

doi: 10.3978/j.issn.2223-3652.2014.11.06

View this article at: <http://dx.doi.org/10.3978/j.issn.2223-3652.2014.11.06>

Introduction

Arterial calcification has been demonstrated to associate with an increased risk of cardiovascular events (1,2). Calcified plaque has been traditionally considered as a passive degenerative and quiescent form of disease, resulting from similar mechanisms to that of bone development (1). This concept has been supported by previous observations

which plaque calcification is more prevalent in stable patients with coronary artery disease (CAD) (3-5) and is less likely to change despite anti-atherosclerotic medical therapies (6). However, recent molecular imaging studies have shown that arterial calcification can also reflect an active process stimulated by inflammation (7-11). Inflammatory cytokines contributed to early stages of

plaque calcification by activating osteogenic differentiation and mineralization of vascular cells (9). TNF- α has been reported to enhance vascular calcification by promoting osteoblastic differentiation of vascular cells (10). Moreover, in advanced stages of calcification, increased mineralization and decreased macrophages have been associated with limited inflammation (9). These findings suggest that inflammatory pathways play important roles in developing early calcification.

Small amounts of calcium in a spotty distribution have been demonstrated in culprit lesions of patients with acute coronary events (12-15). Previous studies reported increased biomechanical plaque stress due to calcification as a possible mechanism of plaque rupture (16,17). However, given that inflammation contributes to plaque instability in many acute coronary events, the concept that spotty calcification may activate inflammatory cytokines and affect plaque morphology associated with plaque vulnerability has gained increasing support.

Frequency-domain optical coherence tomography (FD-OCT) is an intracoronary imaging modality with a high resolution of 10 to 20 μ m that provides detailed plaque microstructural information contributing to plaque vulnerability (18-22). In the current study, we employed FD-OCT to elucidate the association of spotty calcification and plaque microstructures at non-culprit lesions assessed by FD-OCT imaging in patients with stable CAD.

Materials and methods

Study population

We identified the current study subjects from The Cleveland Clinic FD-OCT Registry. This is a single center prospective registry to enroll clinically stable patients with CAD undertaking FD-OCT imaging for the culprit vessel prior to the scheduled percutaneous coronary intervention (PCI). Patients are eligible for this registry if they are clinically indicated for PCI due to having cardiac ischemic symptom or evidence of suspected cardiac ischemia demonstrated by electrocardiogram, echocardiography or stress exercise test. Patients with acute coronary syndrome, cardiogenic shock, chronic total occlusion within target vessel, congestive heart failure, a left main disease, a history of PCI within the culprit vessel and renal failure are not enrolled. The current study included patients with analyzable FD-OCT images of non-culprit lipid-rich plaques within the target vessel for PCI. Of 308 patients

in this registry, we excluded 3 patients due to poor image quality and 5 patients having lesions in bypass grafts. The remaining 300 stable CAD patients were analyzed in the current study. The study was approved by the institutional review board committee at the Cleveland Clinic and all patients gave written informed consent before enrollment.

FD-OCT data acquisition

Intravascular FD-OCT imaging of the entire target vessel was performed prior to PCI as previously described (23). Briefly, following intracoronary administration of nitroglycerin (0.5 mg), a FD-OCT (C7-XRTM OCT Intravascular Imaging System; St. Jude Medical, St. Paul, Minnesota) was advanced to the distal site of the target artery. The FD-OCT pullback was performed at 20 mm/s during the continuous injection of contrast media through the guiding catheter. Multiple FD-OCT pullbacks were required to image the entire of target vessel. Each FD-OCT imaged segment was overlapped by using a side branch as a landmark. The raw FD-OCT data were anonymized and transferred to open-source software, ImageJ (National Institutes of Health, Bethesda, Maryland). All FD-OCT images were analyzed at Atherosclerosis Imaging Core Laboratory of Cleveland Clinic by experienced investigators who were blinded to the clinical presentations. Any discrepancies between the observers were resolved by consensus.

FD-OCT data analysis

Non-culprit lipid plaques with diameter stenosis between 20% and 70% were analyzed. Culprit lesions were identified by angiographic, electrocardiographic and echocardiographic findings and non-invasive stress test result. The non-culprit plaques were defined as any lesions where PCI was not performed. Each plaque was separated by at least 5 mm from the edge of any other plaque or implanted stent edge. Lipid arc was measured in every cross-sectional frame and then averaged. Lipid length was recorded on a longitudinal view. Lipid index was defined as the mean lipid arc multiplied by lipid length (24-27). Calcification was defined as an area with low backscattering signal and a sharp border within a plaque (23). Spotty calcification was defined as the presence of lesions <4 mm in length and containing an arc of calcification <90° according to the definition of previous studies using grayscale intravascular ultrasound (12,28) (*Figure 1*). The number of

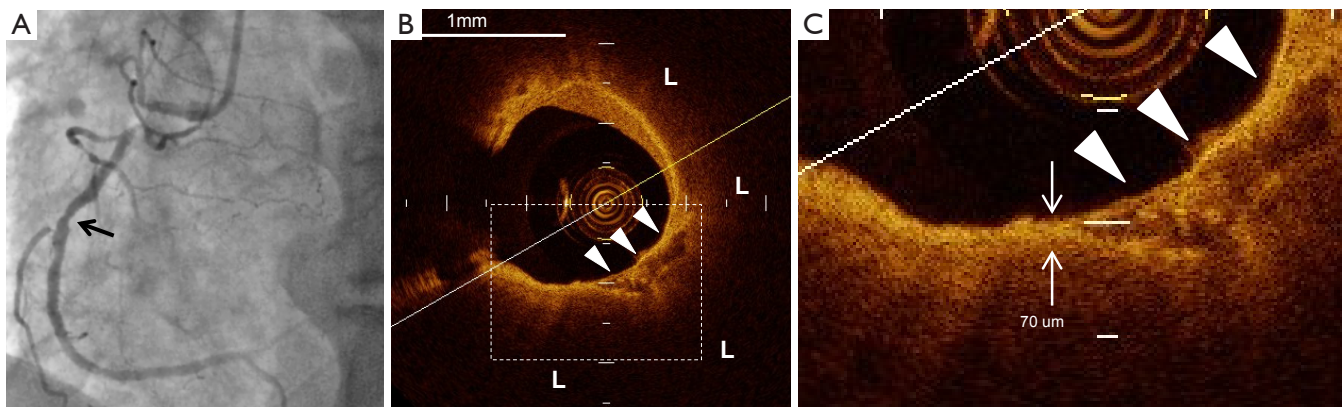


Figure 1 The representative images of plaque containing spotty calcification. (A) Coronary angiography demonstrated a non-culprit lesion at mid of the right coronary artery (arrow); (B) the corresponding FD-OCT image presents spotty calcification (arrow heads) within lipid plaque (L); (C) the thinnest fibrous cap (short arrow) was observed close to spotty calcification (arrow heads). Its thickness was 70 μm . FD-OCT, frequency-domain optical coherence tomography.

spotty calcification within plaque was counted. The fibrous cap thickness was defined as the minimum distance from the coronary artery lumen to inner border of lipid (23). The average of three measurements at its thinnest part was used for the analysis. Thin-cap fibroatheroma was defined as a plaque with lipid content in ≥ 2 quadrants and the thinnest part of fibrous cap thickness $\leq 65 \mu\text{m}$ (23). A microchannel was defined as signal-poor voids without a connection to the vessel lumen recognized on more than three consecutive cross-sectional OCT frames (22,23). Plaque rupture was defined as the presence of fibrous cap discontinuity and cavity formation in the plaque (23). Intracoronary thrombus was identified as a mass protruding into the vessel lumen from the surface of the vessel wall (23). Macrophage was defined as linear high-intensity signals on plaque surfaces accompanied by high attenuation. The inter- and intra-observer differences for the measurements of calcium arc were $1.2^\circ \pm 1.0^\circ$ and $1.8^\circ \pm 1.5^\circ$, respectively. Intraobserver and interobserver correlation coefficients for the measurement of calcium arc were 0.99 and 0.96, respectively. The inter- and intra-observer correlation coefficients and differences for the measurement of fibrous cap thickness were 0.90 and 0.96, and 18 ± 16 and $13 \pm 11 \mu\text{m}$, respectively.

Statistical analysis

Continuous variables are expressed as mean \pm SD, and categorical variables as numbers and percentage. The Chi-square test was used to test for differences in categorical variables between groups and continuous data were

compared using unpaired *t*-tests or Mann-Whitney log rank tests when the variable was not normally distributed. Relations between the maximum number of spotty calcification and fibrous cap thickness were analyzed by Spearman's correlation coefficients. To compare FD-OCT measures in plaques with and without spotty calcification, Generalized Estimating Equations approach were used to take into account the intraclass correlation due to the multiple plaques analyzed within a single patient's data. A value of $P < 0.05$ was considered significant. All statistical analyses were performed using SAS software, version 9.1.3 (SAS Institute, Cary North Carolina).

Results

Patients' demographics

Totally 123 patients (41.0%) had spotty calcification within non-culprit lipid plaques. Baseline clinical characteristics are summarized in *Table 1*. Patients with spotty calcification were less likely to be obese. The use of anti-atherosclerotic medical therapies and biochemistry measures are shown in *Table 2*. Patients with spotty calcification had higher triglyceride and lower high-density lipoprotein cholesterol levels.

FD-OCT measures at non-culprit plaques containing spotty calcification

We conducted single, double and triple vessel FD-OCT

Table 1 Baseline patients' clinical characteristics

| Variables | Patients without spotty calcification (n=185) | Patients with spotty calcification (n=123) | P value |
|---|---|--|---------|
| Age (years) | 61.5±11.3 | 62.1±9.6 | 0.51 |
| Male (%) | 140 (75.7) | 92 (74.8) | 0.75 |
| BMI (kg/m ²) | 31.2±6.3 | 28.5±4.3 | 0.004 |
| Hypertension, n (%) | 130 (70.3) | 89 (72.4) | 0.80 |
| Hyperlipidemia, n (%) | 129 (69.7) | 90 (73.2) | 0.71 |
| Diabetes, n (%) | 64 (34.6) | 45 (36.6) | 0.80 |
| Current smoker, n (%) | 23 (12.4) | 17 (13.8) | 0.85 |
| Metabolic syndrome | 78 (42.2) | 49 (39.8) | 0.79 |
| A history of myocardial infarction, n (%) | 42 (22.7) | 41 (33.3) | 0.95 |
| A history of PCI, n (%) | 34 (18.4) | 21 (17.1) | 0.87 |
| A history of CABG, n (%) | 3 (1.6) | 3 (2.4) | 0.92 |
| Single vessel disease, n (%) | 136 (73.5) | 92 (74.8) | 0.87 |
| Double vessel disease, n (%) | 39 (21.1) | 22 (17.9) | 0.72 |
| Triple vessel disease, n (%) | 10 (5.4) | 9 (7.3) | 0.82 |

BMI, body mass index; CABG, coronary artery bypass grafting.

Table 2 Biochemistry data

| Variables | Patients without spotty calcification (n=185) | Patients with spotty calcification (n=123) | P value |
|--------------------------------|---|--|---------|
| Medication | | | |
| Aspirin, n (%) | 184 (99.5) | 123 (100.0) | 0.98 |
| Statin, n (%) | 155 (83.8) | 104 (84.6) | 0.92 |
| β blockers, n (%) | 130 (70.3) | 90 (73.2) | 0.72 |
| ACE inhibitor, n (%) | 86 (46.5) | 67 (54.5) | 0.32 |
| ARB, n (%) | 26 (14.1) | 12 (9.8) | 0.60 |
| Calcium channel blocker, n (%) | 41 (22.2) | 20 (16.3) | 0.40 |
| Biochemistry data | | | |
| Total cholesterol (mmol/L) | 4.4±1.2 | 4.4±1.1 | 0.96 |
| Triglyceride (mmol/L) | 1.1 (0.8, 1.7) | 1.4 (0.8, 2.8) | 0.006 |
| LDL-C (mmol/L) | 2.5±1.0 | 2.4±0.8 | 0.55 |
| HDL-C (mmol/L) | 1.2±0.3 | 1.0±0.3 | 0.04 |
| Fasting glucose (mmol/L) | 6.9±3.5 | 7.2±2.6 | 0.59 |
| Systolic BP (mmHg) | 131.4±13.6 | 138.2±14.7 | 0.83 |
| Diastolic BP (mmHg) | 82.3±8.9 | 85.5±8.3 | 0.88 |

ACE, angiotensin converting enzyme; ARB, angiotensin II receptor blocker; BP, blood pressure; HDL-C, high-density lipoprotein cholesterol; LDL-C, low-density lipoprotein cholesterol.

Table 3 FD-OCT imaging procedural data for target vessels

| Variables | Patients without spotty calcification (n=185) | Patients with spotty calcification (n=123) | P value |
|------------------------------|---|--|---------|
| Number of imaged vessels | | | |
| Single vessel, n (%) | 140 (75.7) | 95 (77.2) | 0.85 |
| Double vessel, n (%) | 35 (18.9) | 19 (15.4) | 0.78 |
| Triple vessel, n (%) | 10 (5.4) | 8 (6.5) | 0.89 |
| Averaged number of pullbacks | 2.1±0.5 | 2.3±0.4 | 0.80 |
| Length of imaged vessels | | | |
| LAD (mm) | 85±14 | 82±11 | 0.62 |
| LCX (mm) | 48±11 | 52±10 | 0.50 |
| RCA (mm) | 90±21 | 88±18 | 0.75 |

FD-OCT, frequency-domain optical coherence tomography; LAD, left anterior descending artery; LCX, left circumflex artery; RCA, right coronary artery.

imaging in 229, 52 and 18 patients, respectively (*Table 3*). Throughout these imaging procedures, 280 non-culprit lipid plaques were identified in the 387 target vessels requiring PCI. 39.6% (111/280) of these plaques contained at least one spotty calcification. About 30.6% (34/111) of those had multiple spotty calcifications within plaque. Plaque-based analysis of FD-OCT measures in non-culprit lipid plaques with and without spotty calcification is summarized in *Table 4*. FD-OCT imaging demonstrated that plaques with spotty calcification had larger lipid burden reflected by lipid length and lipid index. Thinner fibrous cap thickness and a higher prevalence of microchannels and macrophages were also observed at non-culprit lipid plaques with spotty calcification. The prevalence of thin-cap fibroatheroma and plaque rupture was higher in patients with spotty calcification although these were statistically non-significant. A significant association was observed between the number of spotty calcifications and fibrous cap thickness (*Figure 2*). Increased number of spotty calcification was also associated with higher prevalence of microchannel within plaque (*Figure 3*).

The inter- and intra-observer differences for the measurements of calcium arc were $1.2^\circ \pm 1.0^\circ$ and $1.8^\circ \pm 1.5^\circ$, respectively. Intraobserver and interobserver correlation coefficients for the measurement of calcium arc were 0.99 and 0.96, respectively. The inter- and intra-observer correlation coefficients and differences for the measurement of fibrous cap thickness were 0.90 and 0.96, and 18 ± 16 and 13 ± 11 μm , respectively.

Statin and fibrous cap thickness of plaques containing spotty calcium

The association of statin therapy with fibrous cap thickness of plaques with and without spotty calcification is summarized in *Figure 4*. The use of a statin was associated with a greater fibrous cap thickness in plaques both with and without spotty calcification.

Discussion

The current study demonstrated that spotty calcified lesions exhibited vulnerable plaque features imaged by FD-OCT. In particular, lesions had thinner fibrous cap if they contained more number of spotty calcification. These findings indicate the association of spotty calcification with plaque microstructural characteristics of plaque vulnerability.

Recently, vascular calcification has been considered an active participant in plaque development through its action on macrophages. Secretion of the inflammatory cytokines from macrophages promotes osteogenic transformation of vascular cells and generates microcalcification (11,29-31). In addition, a positive feed-back loop further stimulating macrophage activation and mineralization produces spotty calcification (7,32). Since macrophages render plaques vulnerable to rupture (33,34), the macrophage-triggered formation of spotty calcification would potentially promote plaque vulnerability. In the current study, the presence of spotty calcium within plaques was associated with larger

Table 4 FD-OCT derived measures in plaques with spotty calcification

| Variables | Plaques without spotty calcification (183 lipid plaques) | Plaques with spotty calcification (111 lipid plaques) | P value |
|---|---|--|---------|
| Plaque location | | | |
| LAD, n (%) | 87 (47.5) | 59 (53.2) | 0.52 |
| LCX, n (%) | 46 (25.1) | 30 (27.0) | 0.79 |
| RCA, n (%) | 50 (27.3) | 22 (19.8) | 0.39 |
| QCA parameters | | | |
| Reference diameter (mm) | 3.4±0.4 | 3.2±0.3 | 0.85 |
| Minimum lesion diameter (mm) | 1.4±0.2 | 1.2±0.3 | 0.88 |
| Percent diameter stenosis (%) | 39.1±15.4 | 38.4±12.7 | 0.65 |
| FD-OCT derived measures | | | |
| Average lipid arc (°) | 171.5±91.8 | 210.3±92.0 | 0.06 |
| Lipid length (mm) | 4.8±5.1 | 8.9±7.2 | 0.001 |
| Lipid index (mm°) | 815.2±1,040.3 | 1,711.8±1,522.3 | <0.0001 |
| Fibrous cap thickness (μm) | 112.5±32.5 | 89.0±31.6 | 0.002 |
| Thin-cap fibroatheroma, n (%) | 28 (15.3) | 32 (28.8) | 0.15 |
| Plaque rupture, n (%) | 17 (9.3) | 23 (20.7) | 0.06 |
| Thrombus, n (%) | 1 (0.5) | 4 (3.6) | 0.69 |
| Macrophage (%) | 37 (20.2) | 53 (47.7) | <0.0001 |
| Spotty calcification | | | |
| Spotty calcium number per plaques, n | – | 1.4±0.7 | – |
| Spotty calcium length per plaques (mm) | – | 1.3±0.9 | – |
| Average arc of spotty calcium (°) | – | 31.6±12.8 | – |
| FD-OCT, frequency-domain optical coherence tomography; LAD, left anterior descending artery; LCX, left circumflex artery; RCA, right coronary artery. | | | |

lipid burden, thinner fibrous cap and higher frequency of microchannels. Considering that activated macrophages contribute to plaque growth, thinning fibrous cap and inducing angiogenesis via secreted proinflammatory cytokines (35–38), the FD-OCT derived vulnerable feature of spotty calcified lesions might underscore the early plaque calcification contributing to plaque instability.

Multiple depositions of spotty calcification were associated with more profound vulnerable features. Previous studies using grayscale intravascular ultrasound reported that ruptured plaques and culprit lesions causing acute myocardial infarction are more likely to contain greater number of small calcium deposits which are short in length (12,39). The formation of microcalcification has been shown to provoke additional proinflammatory responses, thereby stimulating plaque calcification (7,32). As such, a greater number of spotty calcium would induce

more activated inflammation responses, leading to further destabilizing plaques.

The current study also demonstrates the potential importance of spotty calcium even in patients with stable CAD, despite most reports focusing on patients with acute coronary syndrome. FD-OCT imaging identified spotty calcification at non-culprit lesions in 41% of stable patients. Other studies using intravascular ultrasound and multi-slice computed tomography have reported that 27% and 43% of stable patients had spotty calcification at non-culprit lesions, respectively (28,40). These findings suggest that spotty calcification is not a rare plaque microstructure at non-culprit lesions in patients with stable CAD. The possible role of spotty calcification as an important feature of plaque vulnerability in risk stratification of future ischemic events needs to be addressed.

Coronary artery calcification has been considered

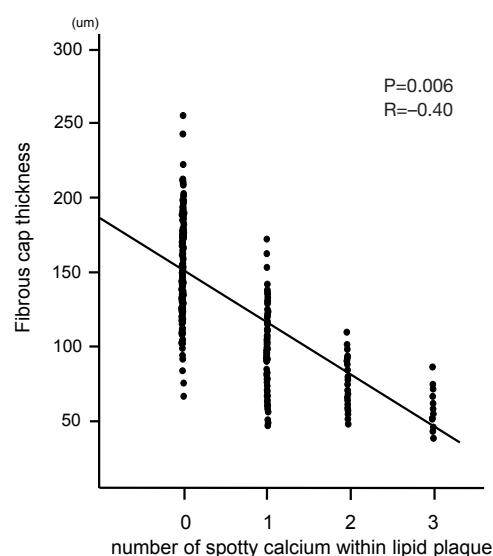


Figure 2 The correlation between the number of spotty calcification and fibrous cap thickness. The number of spotty calcification was counted within each plaque. The fibrous cap thickness was defined as the minimum distance from the coronary artery lumen to inner border of lipid. The average of three measurements at its thinnest part was used for the analysis.

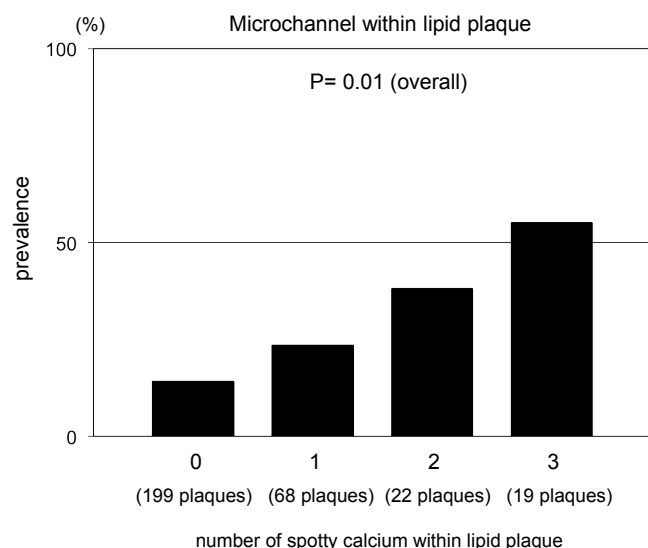


Figure 3 Microchannel and the number of spotty calcification. Prevalence of microchannel in plaques stratified according to the number of spotty calcification. The number of spotty calcification was counted within each plaque.

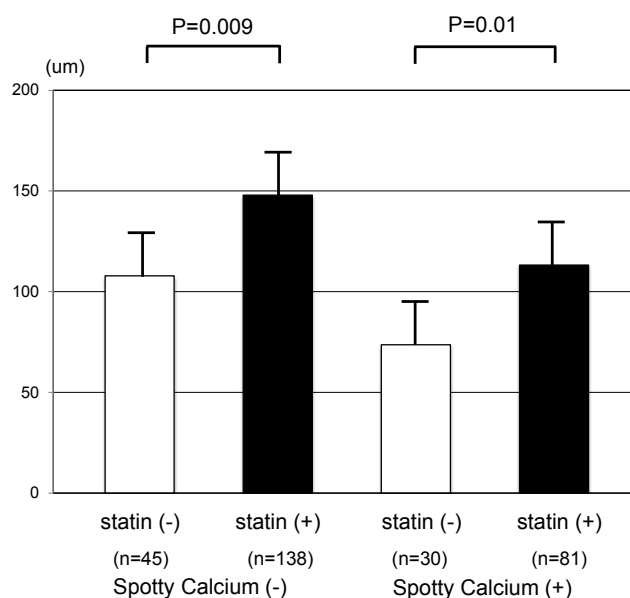


Figure 4 Statin therapy and fibrous cap thickness. Fibrous cap thickness of plaques with and without spotty calcification stratified according to a statin.

to be resistant to statin therapy. Previous clinical trials failed to prove the benefit of lowering LDL-C level by a potent statin therapy in halting progression of coronary artery calcification (41,42). We have already reported that calcified plaques are less likely to changes in atheroma burden under medical therapies including a statin (6). These observations indicate difficulty in modifying calcified lesions by medical therapies. However, the current analysis showed that fibrous cap at spotty calcified plaques favourably responded to a statin. Recent study has demonstrated that spotty calcification is not quiescent but an active stage of atherosclerosis associated with inflammation (7). Given that a statin has the ability of modulating inflammatory activities, this property might contribute to favourable modification of fibrous cap even at lesions containing spotty calcification. As such, the current observation suggests that spotty calcified plaques might be amenable to statin therapy. Also, this plaque phenotype may be an important therapeutic target which requires a statin to stabilize lesions, potentially leading to the prevention of future cardiovascular events.

A number of caveats should be noted. We can not

exclude the possibility of selection bias because patients in our registry were selected for FD-OCT imaging by the operator. Due to its shallow penetration depth of the infra-red light beam, FD-OCT does not have enough capabilities to measure necrotic core and plaque burden. Also, shallow axial penetration of FD-OCT leads to missing some compositional data, especially at the bottom level of plaque. Although we used lipid index to evaluate lipid amount within non-culprit plaques [25-27], this index was not fully established and validated against histological data. All patients underwent FD-OCT imaging in the setting of a clinically indicated PCI. It is unknown whether similar findings would be observed in asymptomatic individuals.

In summary, non-culprit lipid-rich plaques containing spotty calcification exhibited vulnerable FD-OCT features in patients with stable CAD requiring PCI. The greater number of spotty calcification was associated with thinner fibrous cap at non-culprit lipid-rich plaques. Our findings may indicate the contribution of spotty calcification to the enhanced plaque vulnerability.

Acknowledgements

The authors are grateful for the technical expertise of the Atherosclerosis Imaging Core Laboratory of the Cleveland Clinic.

Disclosure: Steven E. Nissen has received research support to perform clinical trials through the Cleveland Clinic Coordinating Center for Clinical Research from Pfizer, AstraZeneca, Novartis, Roche, Daiichi-Sankyo, Takeda, Sanofi-Aventis, Resverlogix, and Eli Lilly; and is a consultant/advisor for many pharmaceutical companies but requires them to donate all honoraria or consulting fees directly to charity so that he receives neither income nor a tax deduction. Stephen J Nicholls has received speaking honoraria from AstraZeneca, Pfizer, Merck Schering-Plough and Takeda, consulting fees from AstraZeneca, Pfizer, Merck Schering-Plough, Takeda, Roche, NovoNordisk, LipoScience and Anthera and research support from AstraZeneca and Lipid Sciences. Other authors declare no conflict of interest.

References

- Wallin R, Wajih N, Greenwood GT, et al. Arterial calcification: a review of mechanisms, animal models, and the prospects for therapy. *Med Res Rev* 2001;21:274-301.
- Abedin M, Tintut Y, Demer LL. Vascular calcification: mechanisms and clinical ramifications. *Arterioscler Thromb Vasc Biol* 2004;24:1161-70.
- Beckman JA, Ganz J, Creager MA, et al. Relationship of clinical presentation and calcification of culprit coronary artery stenoses. *Arterioscler Thromb Vasc Biol* 2001;21:1618-22.
- Nakamura M, Nishikawa H, Mukai S, et al. Impact of coronary artery remodeling on clinical presentation of coronary artery disease: an intravascular ultrasound study. *J Am Coll Cardiol* 2001;37:63-9.
- Shemesh J, Stroh CI, Tenenbaum A, et al. Comparison of coronary calcium in stable angina pectoris and in first acute myocardial infarction utilizing double helical computerized tomography. *Am J Cardiol* 1998;81:271-5.
- Nicholls SJ, Tuzcu EM, Wolski K, et al. Coronary artery calcification and changes in atheroma burden in response to established medical therapies. *J Am Coll Cardiol* 2007;49:263-70.
- Aikawa E, Nahrendorf M, Figueiredo JL, et al. Osteogenesis associates with inflammation in early-stage atherosclerosis evaluated by molecular imaging in vivo. *Circulation* 2007;116:2841-50.
- Demer LL, Tintut Y. Vascular calcification: pathobiology of a multifaceted disease. *Circulation* 2008;117:2938-48.
- New SE, Aikawa E. Molecular imaging insights into early inflammatory stages of arterial and aortic valve calcification. *Circ Res* 2011;108:1381-91.
- Tintut Y, Patel J, Parhami F, et al. Tumor necrosis factor- α promotes in vitro calcification of vascular cells via the cAMP pathway. *Circulation* 2000;102:2636-42.
- Radcliff K, Tang TB, Lim J, et al. Insulin-like growth factor-I regulates proliferation and osteoblastic differentiation of calcifying vascular cells via extracellular signal-regulated protein kinase and phosphatidylinositol 3-kinase pathways. *Circ Res* 2005;96:398-400.
- Ehara S, Kobayashi Y, Yoshiyama M, et al. Spotty calcification typifies the culprit plaque in patients with acute myocardial infarction: an intravascular ultrasound study. *Circulation* 2004;110:3424-9.
- Motoyama S, Kondo T, Sarai M, et al. Multislice computed tomographic characteristics of coronary lesions in acute coronary syndromes. *J Am Coll Cardiol* 2007;50:319-26.

14. Kolodgie FD, Burke AP, Farb A, et al. The thin-cap fibroatheroma: a type of vulnerable plaque: the major precursor lesion to acute coronary syndromes. *Curr Opin Cardiol* 2001;16:285-92.
15. Burke AP, Weber DK, Kolodgie FD, et al. Pathophysiology of calcium deposition in coronary arteries. *Herz* 2001;26:239-44.
16. Bluestein D, Alemu Y, Avrahami I, et al. Influence of microcalcifications on vulnerable plaque mechanics using FSI modeling. *J Biomech* 2008;41:1111-8.
17. Kelly-Arnold A, Maldonado N, Laudier D, et al. Revised microcalcification hypothesis for fibrous cap rupture in human coronary arteries. *Proc Natl Acad Sci U S A* 2013;110:10741-6.
18. Huang D, Swanson EA, Lin CP, et al. Optical coherence tomography. *Science* 1991;254:1178-81.
19. Jang IK, Bouma BE, Kang DH, et al. Visualization of coronary atherosclerotic plaques in patients using optical coherence tomography: comparison with intravascular ultrasound. *J Am Coll Cardiol* 2002;39:604-9.
20. Yun SH, Tearney GJ, Vakoc BJ, et al. Comprehensive volumetric optical microscopy in vivo. *Nat Med* 2006;12:1429-33.
21. Tearney GJ, Waxman S, Shishkov M, et al. Three-dimensional coronary artery microscopy by intracoronary optical frequency domain imaging. *JACC Cardiovasc Imaging* 2008;1:752-61.
22. Kitabata H, Tanaka A, Kubo T, et al. Relation of microchannel structure identified by optical coherence tomography to plaque vulnerability in patients with coronary artery disease. *Am J Cardiol* 2010;105:1673-8.
23. Tearney GJ, Regar E, Akasaka T, et al. Consensus standards for acquisition, measurement, and reporting of intravascular optical coherence tomography studies: a report from the International Working Group for Intravascular Optical Coherence Tomography Standardization and Validation. *J Am Coll Cardiol* 2012;59:1058-72.
24. Yabushita H, Bouma BE, Houser SL, et al. Characterization of human atherosclerosis by optical coherence tomography. *Circulation* 2002;106:1640-5.
25. Kato K, Yonetsu T, Kim SJ, et al. Nonculprit plaques in patients with acute coronary syndromes have more vulnerable features compared with those with non-acute coronary syndromes: a 3-vessel optical coherence tomography study. *Circ Cardiovasc Imaging* 2012;5:433-40.
26. Kato K, Yonetsu T, Kim SJ, et al. Comparison of nonculprit coronary plaque characteristics between patients with and without diabetes: a 3-vessel optical coherence tomography study. *JACC Cardiovasc Interv* 2012;5:1150-8.
27. Kato K, Yonetsu T, Jia H, et al. Nonculprit coronary plaque characteristics of chronic kidney disease. *Circ Cardiovasc Imaging* 2013;6:448-56.
28. Kataoka Y, Wolski K, Uno K, et al. Spotty calcification as a marker of accelerated progression of coronary atherosclerosis: insights from serial intravascular ultrasound. *J Am Coll Cardiol* 2012;59:1592-7.
29. Tintut Y, Patel J, Parhami F, et al. Tumor necrosis factor- α promotes in vitro calcification of vascular cells via the cAMP pathway. *Circulation* 2000;102:2636-42.
30. Shioi A, Katagi M, Okuno Y, et al. Induction of bone-type alkaline phosphatase in human vascular smooth muscle cells: roles of tumor necrosis factor- α and oncostatin M derived from macrophages. *Circ Res* 2002;91:9-16.
31. Watson KE, Boström K, Ravindranath R, et al. TGF- β 1 and 25-hydroxycholesterol stimulate osteoblast-like vascular cells to calcify. *J Clin Invest* 1994;93:2106-13.
32. Aikawa E. Optical Molecular Imaging of Inflammation and Calcification in Atherosclerosis. *Curr Cardiovasc Imaging Rep* 2010;3:12-7.
33. Moore KJ, Sheedy FJ, Fisher EA. Macrophages in atherosclerosis: a dynamic balance. *Nat Rev Immunol* 2013;13:709-21.
34. Moldovan NI, Goldschmidt-Clermont PJ, Parker-Thornburg J, et al. Contribution of monocytes/macrophages to compensatory neovascularization: the drilling of metalloelastase-positive tunnels in ischemic myocardium. *Circ Res* 2000;87:378-84.
35. Kumar AH, Martin K, Turner EC, et al. Role of CX3CR1 receptor in monocyte/macrophage driven neovascularization. *PLoS One* 2013;8:e57230.
36. Tabas I. Consequences and therapeutic implications of macrophage apoptosis in atherosclerosis: the importance of lesion stage and phagocytic efficiency. *Arterioscler Thromb Vasc Biol* 2005;25:2255-64.
37. Lendon CL, Davies MJ, Born GV, et al. Atherosclerotic plaque caps are locally weakened when macrophages density is increased. *Atherosclerosis* 1991;87:87-90.
38. Shah PK, Falk E, Badimon JJ, et al. Human monocyte-derived macrophages induce collagen breakdown in fibrous caps of atherosclerotic plaques. Potential role of matrix-degrading metalloproteinases and implications for plaque

- rupture. *Circulation* 1995;92:1565-9.
39. Fujii K, Carlier SG, Mintz GS, et al. Intravascular ultrasound study of patterns of calcium in ruptured coronary plaques. *Am J Cardiol* 2005;96:352-7.
 40. Shmilovich H, Cheng VY, Tamarappoo BK, et al. Vulnerable plaque features on coronary CT angiography as markers of inducible regional myocardial hypoperfusion from severe coronary artery stenoses. *Atherosclerosis* 2011;219:588-95.
 41. Schmermund A, Achenbach S, Budde T, et al. Effect of intensive versus standard lipid-lowering treatment with atorvastatin on the progression of calcified coronary atherosclerosis over 12 months: a multicenter, randomized, double-blind trial. *Circulation* 2006;113:427-37.
 42. Raggi P, Davidson M, Callister TQ, et al. Aggressive versus moderate lipid-lowering therapy in hypercholesterolemic postmenopausal women: Beyond Endorsed Lipid Lowering with EBT Scanning (BELLES). *Circulation* 2005;112:563-71.

Cite this article as: Kataoka Y, Puri R, Hammadah M, Duggal B, Uno K, Kapadia SR, Tuzcu EM, Nissen SE, Nicholls SJ. Spotty calcification and plaque vulnerability *in vivo*: frequency-domain optical coherence tomography analysis. *Cardiovasc Diagn Ther* 2014;4(6):460-469. doi: 10.3978/j.issn.2223-3652.2014.11.06